Materials Transactions, Vol. 51, No. 11 (2010) pp. 2049 to 2055

Factors Influencing Tensile Ductility of OFHC Cu Having Different Ultrafine Grained Structures

Lee Ju Park[1], Hyung Won Kim[1], Chong Soo Lee[2] and Kyung-Tae Park[3,*]

[1]*Agency for Defense Development, P.O. Box 35-42, Taejon 305-600, Korea*
[2]*Department of Materials Science & Engineering, POSTECH, Pohang 790-784, Korea*
[3]*Division of Advanced Materials Science & Engineering, Hanbat National University, Taejon 305-719, Korea*

Tensile ductility of OFHC Cu with the different ultrafine grained (UFG) structures, which were fabricated by the different routes of equal channel angular pressing (ECAP), was associated in detail with the microstructural characteristics developed by ECAP. OFHC Cu having the lamellar and equiaxed UFG structures was prepared by ECAP of routes A and B_c, respectively up to 8 and 16 passes. Their microstructures were closely examined by transmission electron microscopy and orientation image mapping. Tensile tests at room temperature were conducted on the ECAPed samples under the quasi-static condition of $10^{-3}\,s^{-1}$ and $1\,s^{-1}$. Uniform elongation of the lamellar UFG samples decreased with increasing the ECAP passage while both uniform and total elongations of the equiaxed UFG samples increased. In the case of route A producing the lamellar UFG structure, the fractions of high angle grain boundaries and grains less than 0.5 μm increased significantly but an analysis revealed that the dislocation free length decreased with increasing the ECAP passage. For route B_c resulting in the equiaxed UFG structure, the fraction of high angle grain boundaries increased but the grain size distribution and the dislocation free length remained nearly unchanged with increasing the ECAP passage. From the present experiments and analyses, it was found that tensile ductility of lamellar UFG OFHC Cu is primarily controlled by the dislocation free length and that of the equiaxed one is mainly dependent on the fraction of high angle grain boundaries. [doi:10.2320/matertrans.M2010089]

(Received March 8, 2010; Accepted August 2, 2010; Published October 25, 2010)

Keywords: *oxygen free high conductivity (OFHC) copper, ultrafine grains, equal channel angular pressing, grain morphology, ductility*

1. Introduction

In this study, the factors influencing tensile ductility of a ultrafine grained (UFG) oxygen free high conductivity copper (OFHC Cu) having two different grain morphologies, i.e. the lamellar and the equiaxed, at room temperature are explored and compared. The present investigation was motivated by the following consideration. In spite of their exceptionally high strength, a lack of ductility of UFG materials compared to that of coarse grained counterparts is the main drawback for them to be the potential advanced structural materials. There have been several suggestions to extend ductility of UFG materials.[1–7] A common consensus is that a high fraction of high angle grain boundaries (HAGBs) is essential for better ductility. In addition to this common consensus, utilization of partial recrystallization,[1–3] strain gradient plasticity,[4] the second phase particles[5] is also suggested to be helpful to enhance ductility of UFG materials. Interestingly, these suggestions are focused mostly on UFG materials consisting of equiaxed grains. This is primarily because of their isotropic nature relevant to the structural use.

Meanwhile, non-equiaxed UFG materials with anisotropic nature might be beneficial to some special structural applications where the mechanical response highly depends on the loading direction such as high strain rate impact loading: for example, the armor materials and its contradictory (i.e. the penetrator) in military and/or petroleum industries.[8] Regarding the mechanical properties of non-equiaxed UFG materials, Haouaoui *et al.*[9] reported that the grain morphology is the most influencing factor on the plastic flow anisotropy of UFG OFHC Cu under quasi-static loading condition. By contrast, Xu *et al.*[10] demonstrated that plastic anisotropy of UFG Al alloys processed by repetitive equal channel angular pressing (ECAP) diminishes after 6 passes regardless of the strain path, i.e. the types of ECAP route. More recently, it was also reported that non-equiaxed UFG Armco iron[11] and 4130 steel[12] having a lamellar structure exhibited enhanced shear band formability with reduced ductility than equiaxed ones. Although these works provide some insight on understanding the mechanical nature of non-equiaxed UFG materials, detailed information on the microstructural factors influencing their mechanical characteristics, especially ductility, is still lack compared to equiaxed ones; the Hall-Petch strengthening universally explains the strength of UFG materials regardless of the grain morphology. Accordingly, in the present study, the two types of UFG OFHC Cu aforementioned were prepared by ECAP and an attempt was made to rationalize their tensile ductility in association with the microstructural characteristics developed by ECAP.

2. Experimental

As-forged OFHC Cu was annealed at 900 C for 1 h, and then subjected to ECAP at room temperature. After machining the annealed OFHC Cu by ϕ18 mm × 130 mm, ECAP was performed with a ram speed of 2 mm/min to 8 and 16 passes. The ECAP core die was designed to yield an effective strain close to 1 per pass: i.e. inner contact angle and outer curvature angle where the two channels having equal cross-section meet are 90° and 20°, respectively.[13] The ECAP routes of A (without sample rotation on successive pass) and B_c (90° rotation of the sample by same sense on successive pass) were employed in order to obtain two different UFG grain morphologies, the lamellar and the equiaxed, respectively.[14–16]

*Corresponding author, E-mail: ktpark@hanbat.ac.kr

Tensile tests at room temperature were carried out on both unECAPed and ECAPed OFHC Cu samples having the gage section of $25.4 \times 6 \times 2\,mm^3$ on a universal testing machine (MTS Model 4484) with the initial strain rates of 10^{-3} and $1\,s^{-1}$. Tensile specimens were machined such that the tensile axis is parallel to the longitudinal axis of the ECAPed sample. By such, the tensile direction is nearly along with the longitudinal direction of the lamella in the sample processed by route A. At least three specimens were tested at the same strain rate. Microstructures of the ECAPed OFHC Cu were examined by transmission electron microscopy (TEM, JEOL 1010 at 200 kV) through routine metallographic preparation. The distributions of the grain size and grain boundary misorientation were obtained by a scanning electron microscopy (SEM, JEOL JSM-7401F) with secondary and backscattered electron mode. Electron back scattered diffraction patterns (EBSDs) were obtained using a Helios nanolab™ 600 with the acceleration voltage of 30 kV and the scanning step size of 25 nm (a confidence index of 0.22∼0.42).

3. Results and Discussion

3.1 Microstructures

The grain size of annealed OFHC Cu before ECAP was ∼1 mm, and most grains contain annealing twins as shown in Fig. 1(a). A pictorial illustration of the sample passage through the ECAP die and the planes to be observed are presented in Fig. 1(b). Figures 1(c) and 1(d) show TEM microstructures on three orthogonal planes of the samples processed by route A of 8 (hereafter, A8 sample) and 16 (hereafter, A16 sample) passes, respectively. Regardless of the number of passage, grains on the Y plane were severely elongated along the longitudinal axis of the sample, showing a lamellar nature. The grain thickness of elongated grains was typically less than ∼200 nm. Due to the shearing characteristics of route A,[17,18] i.e. a non-redundant process, grains on the X and Z planes were rather ellipsoidal and equiaxed, respectively. By contrast, the samples processed by route B_c of 8 (hereafter, B8 sample) and 16 (hereafter, B16 sample) passes exhibited an equiaxed grain structure on all three orthogonal planes as shown in Figs. 1(e) and 1(f), respectively. It is already well-known that, in the case of route B_c, the equiaxed grain shape is formed usually over 4 passes, and the grain boundaries become more high-angled with little change in the grain size by further passage.[19]

The distributions of grain boundary misorientation of the A samples and B samples obtained from orientation image mapping (OIM) are presented in Figs. 2(a) and 2(b), respectively. The HAGB (misorientation angle larger than 15°) fractions of the A8 and B8 samples were ∼37% and ∼53%, respectively. This fact reveals that route B_c is more effective on producing HAGB than route A for 8 passes. However, the HAGB fraction of the A sample increased more rapidly than that of the B sample with increasing the number of passage; it became almost same as ∼66% for the A16 and B16 sample. This finding is consistent with the previous studies for the efficiency of route A than other routes of ECAP on producing the high HAGB fraction when the inner contact angle of the ECAP die channel is 90°.[20,21] The grain

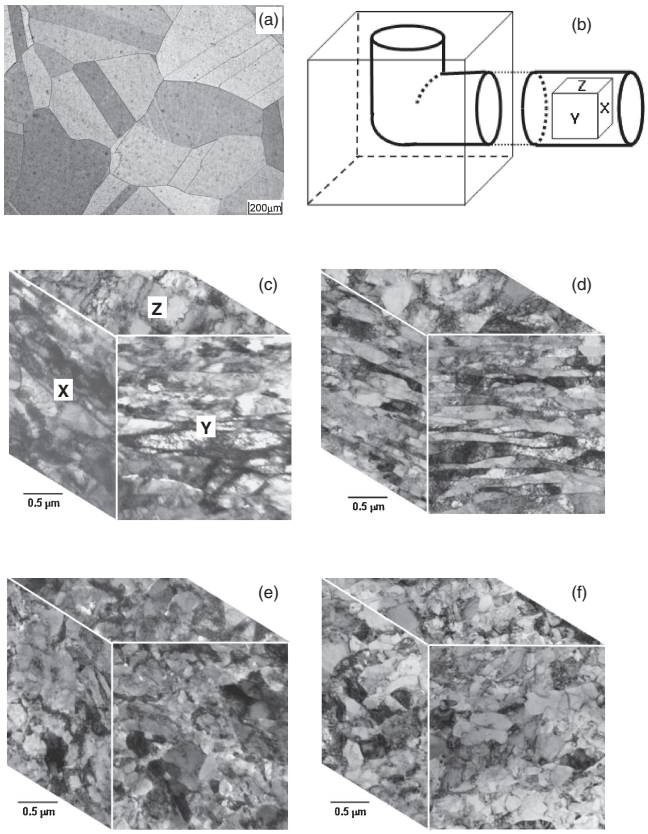

Fig. 1 (a) Optical micrograph of OFHC Cu annealed at 900 C × 1 h; (b) a schematic of the sample passage through a ECAP die and the planes to be observed; (c)∼(f) TEM microstructures on three orthogonal planes of A8, A16, B8 and B16 samples, respectively.

size (in diameter) distributions on the Y plane of the A and B samples are shown in Figs. 2(c) and 2(d), respectively; for the A samples with the lamellar structure, the grain diameter was re-estimated by converting the area of each elongated grain to the diameter of a circular grain. No definite distribution peak was observed in the A8 sample while the A16 sample exhibited the distribution peak at 0.3∼0.4 μm. A fraction of grains smaller than 0.5 μm ($d_{0.5}$) increased significantly with increasing the number of passage, i.e. from ∼28% for the A8 sample to ∼60% for the A16 sample. Both B8 and B16 samples showed the distribution peak around 0.3∼0.4 μm similar to the A16 sample. However, $d_{0.5}$ of the B8 sample (∼79%) was much higher than not only the A8 sample but the A16 sample. It indicates that route B_c is more effective on producing the UFG structure separated by HAGBs than route A. It is of interest to note that $d_{0.5}$ of the B8 sample (∼79%) is almost same with that of the B16 sample (∼77%). This observation informs that grain refinement by route B_c becomes saturated and therefore 8 passes of route B_c is enough to obtain a fairly homogeneous equiaxed UFG structure. The above microstructural characteristics are summarized in Table 1. The OIM images taken on the Y plane of the A and B samples are shown in Fig. 3. The general features of the OIM images are quite comparable with those observed by TEM (Fig. 1(c)∼1(f)). However, the presence of the band structure consisting of elongated subgrains with low angle boundaries was often observed in the A8 sample, for example a region between two dotted lines

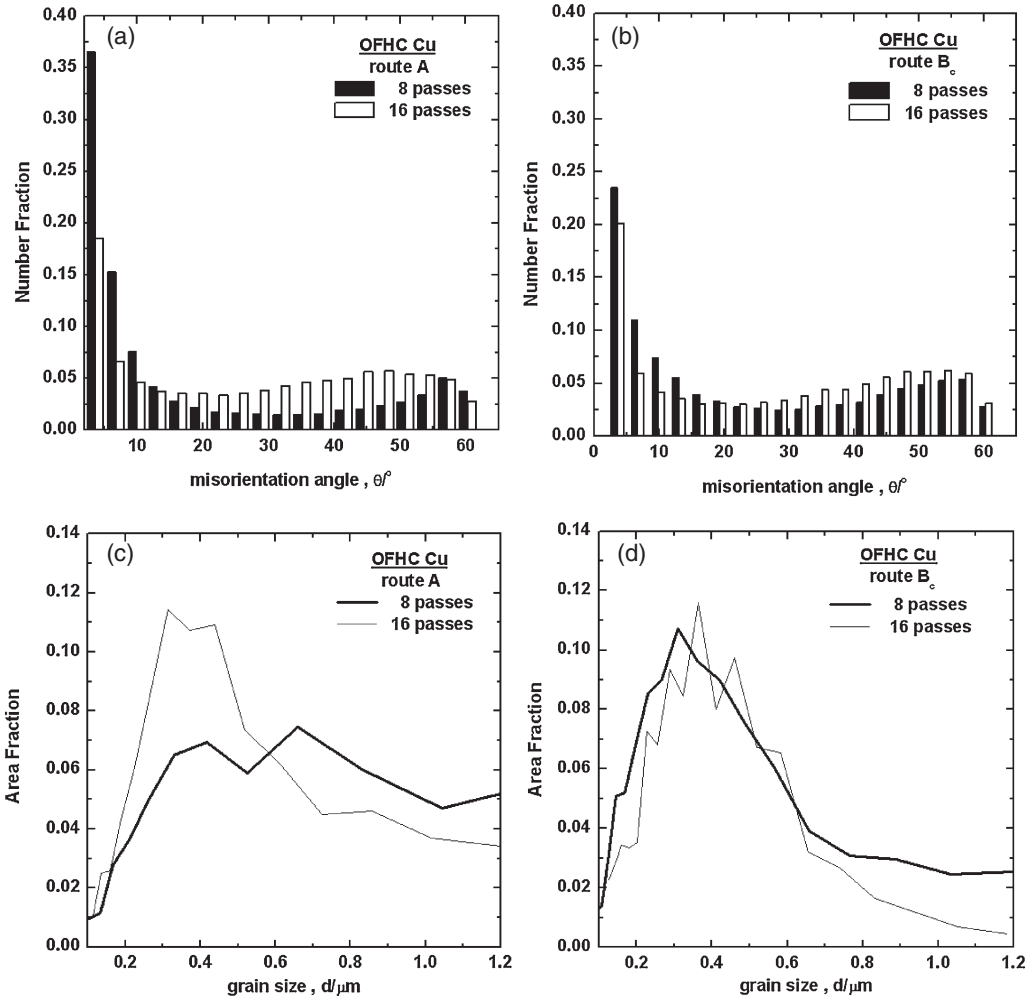

Fig. 2 (a) Distribution of boundary misorientation angle of the A8 and A16 samples; (b) Distribution of boundary misorientation angle of the B8 and B16 samples; (c) Distribution of the grain size in diameter of the A8 and A16 samples; (d) Distribution of the grain size in diameter of the B8 and B16 samples.

Table 1 Mircrostructural characteristics of UFG OFHC Cu processed by ECAP with routes A and B_c.

	A8	A16	B8	B16
HAGB (15° <) fraction	~37%	~66%	~53%	~66%
$d_{0.5}$ fraction	~28%	~60%	~79%	~77%

in Fig. 3(a). The A16 sample (Fig. 3(b)) barely revealed such band structure. Therefore, a large increase of the HAGB and $d_{0.5}$ fractions from the A8 sample to A16 sample is likely to be originated in part from a conversion of low angle boundaries in the band structure to HAGBs. However, even after 16 passes, the $d_{0.5}$ fraction of the A16 sample (~60%) was still much less than that of the B16 sample (~77%) while the HAGB fractions of both are comparable as ~66%.

3.2 Tensile characteristics

The engineering and true stress-strain curves of the A and B samples tensile-tested at room temperature with the initial strain rates of 10^{-3} and $1\,s^{-1}$ are shown in Fig. 4 for 8 passes and Fig. 5 for 16 passes. The nominal tensile properties averaged from three identical tests are listed in

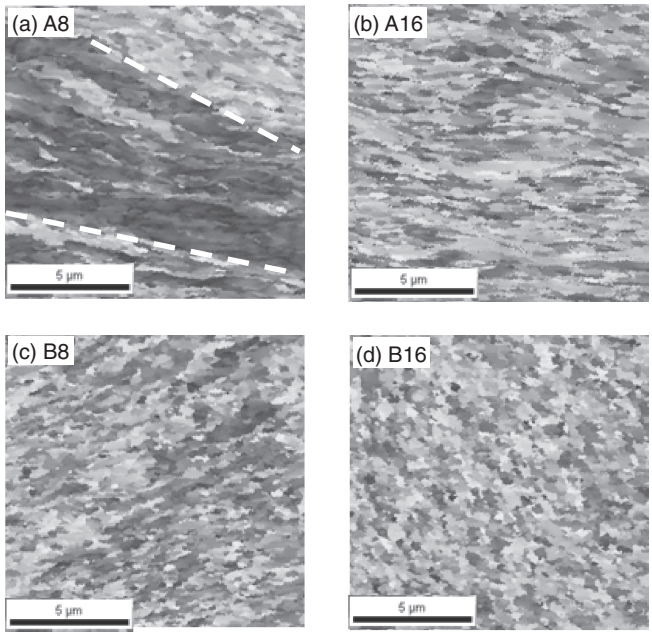

Fig. 3 OIM images taken on the Y plane of ECAPed OFHC Cu: (a) A8 sample; (b) A16 sample; (c) B8 sample; (d) B16 sample.

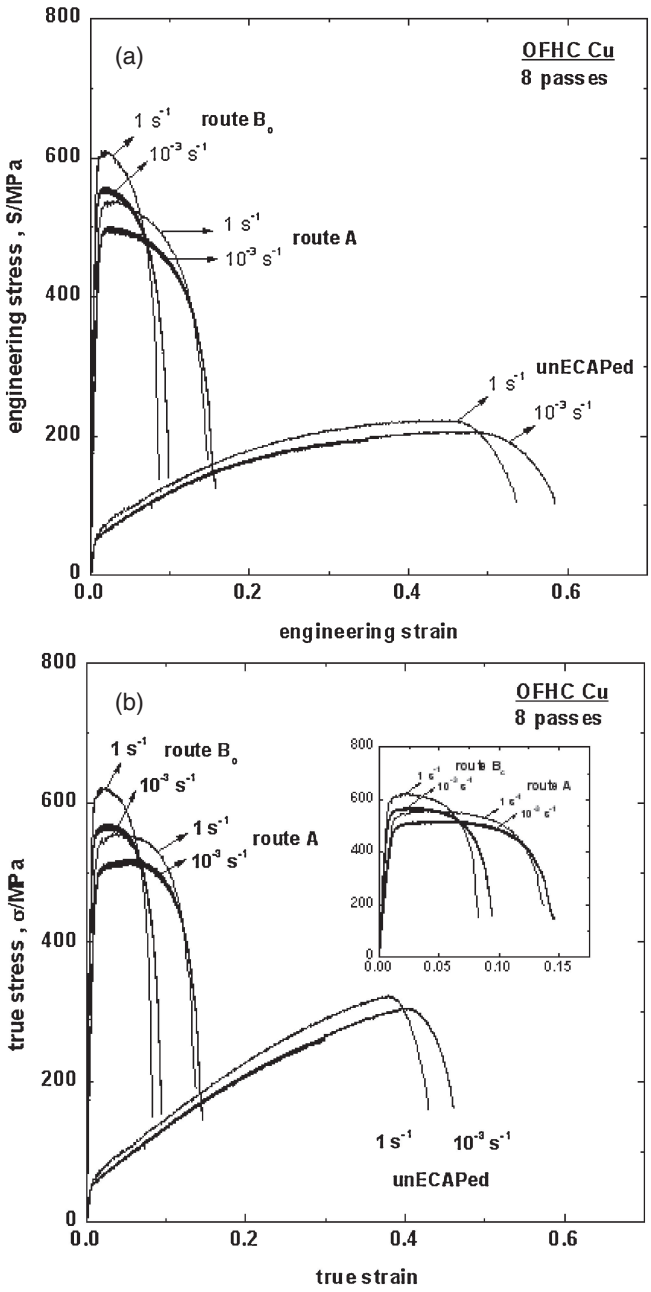

Fig. 4 (a) Engineering and (b) true stress-strain curves of the A8 and B8 samples tensile tested at room temperature with the initial strain rates of 10^{-3} and $1\,s^{-1}$.

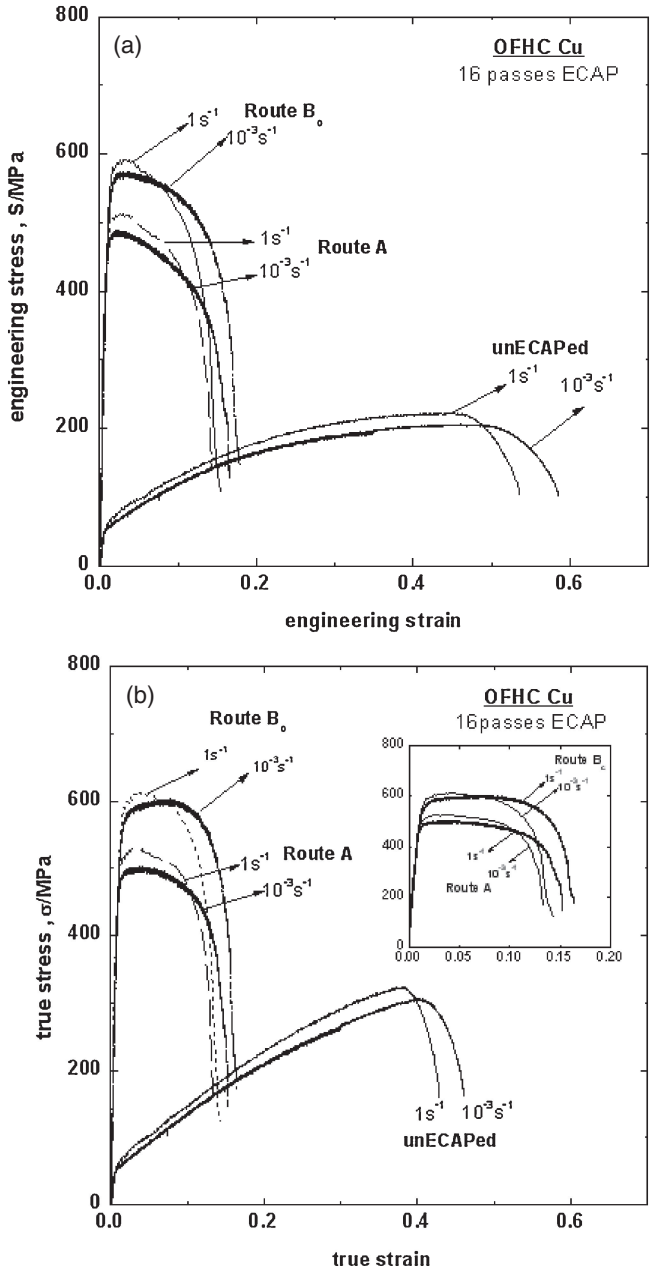

Fig. 5 (a) Engineering and (b) true stress-strain curves of the A16 and B16 samples tensile tested at room temperature with the initial strain rates of 10^{-3} and $1\,s^{-1}$.

Table 2. As typical in UFG materials, the ECAPed samples exhibited the superb yield strength (YS) nearly 10 times higher than that of the unECAPed one, but a drastic loss of ductility. While the yield ratio (YS/UTS) of the unECAPed sample was ~0.25, that of the ECAPed sample was 0.87~0.95, indicating a lack of strain hardenability of the latter. The inferior strain hardenability of the ECAPed samples is more clearly seen by the brief near-perfect plastic behavior in the true stress-strain curves in Figs. 4(b) and 5(b). In addition, regardless of ECAP, the strain rate increase from $10^{-3}\,s^{-1}$ to $1\,s^{-1}$ resulted in the strength increase and ductility loss.

For the purpose of easier comparison, the histograms of the tensile characteristic in Table 2 are constructed in

Table 2 Nominal tensile properties of ECAPed and unECAPed OFHC Cu.

sample	strain rate of $10^{-3}\,s^{-1}$				strain rate of $1\,s^{-1}$			
	YS	UTS	e_u	e_f	YS	UTS	e_u	e_f
unECAPed	49	204	48.1	58.3	56	222	45.1	53.5
A8	461	500	3.6	15.8	496	536	3.4	14.8
A16	463	488	2.4	16.4	472	516	2.8	14.0
B8	520	557	1.6	9.9	580	611	1.4	8.6
B16	512	573	3.4	17.7	516	593	3.2	15.4

YS: yield strength, UTS: ultimate tensile strength, e_u: uniform elongation, e_f: total elongation.
YS and UTS are in MPa; e_u and e_f are in %.

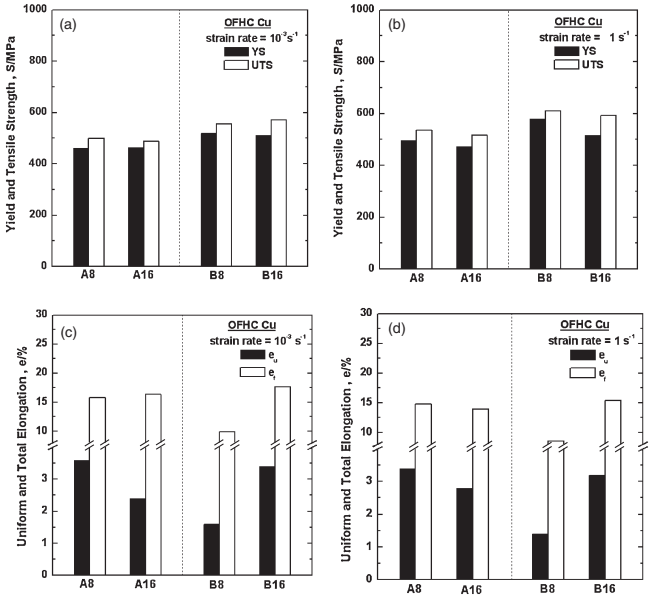

Fig. 6 Histograms showing the comparison of the tensile characteristics of ECAPed OFHC Cu: (a) YS and UTS at 10^{-3} s^{-1}; (b) YS and UTS at 1 s^{-1}; (c) e_u and e_f at 10^{-3} s^{-1}; (d) e_u and e_f at 1 s^{-1}.

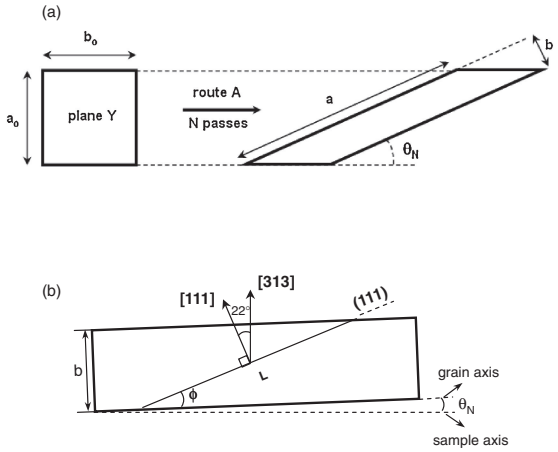

Fig. 7 Pictorial illustrations of (a) geometrical parameters for the configuration change of the element from cubic to lamella as a function of the number of passage for route A,[7] and (b) the orientation relationship between the (111) slip plane and [313] texture with the sample and lamellar grain axes.

Fig. 6. As shown in Figs. 6(a) and 6(b), YS and UTS of the B samples were slightly higher than those of the A samples but the effect of the number of passage on the strength was not significant in the samples processed by the same route, i.e. the saturation of the strengthening effect beyond 8 passes.

For the ductility, as seen in Figs. 6(c) and 6(d), while total elongation (e_f) of the A samples seemed not to be affected by the number of passage, its uniform elongation (e_u) definitely and consistently decreased with increasing the number of passage at both strain rates even though the HAGB faction increased. By contrast, the B samples exhibited the obvious effect of the number of passage on ductility; e_u and e_f of the B16 sample were over 100% and 70% higher respectively than those of the B8 sample at both strain rates.

3.3 Ductility and UFG characteristics

3.3.1 HAGB fraction

From a comparison between Figs. 2 (or Table 1) and 6 (or Table 2), two main facts regarding the effects of microstructural characteristics of UFG OFH Cu processed by the different routes of ECAP on their tensile ductility can be extracted. First, while the HAGB fraction increased significantly from 37% to 66% by increasing the number of passage for the route A, the variation of ductility (e_u and e_f) of the A sample was relatively small; it is reminded that the absolute value of e_u exhibited a small but definite decrease. It indicates that the HAGB fraction is not a critical factor for controlling ductility of a lamellar UFG structure when the lamellar grains are aligned along the tensile direction. Second, both e_u and e_f of the B sample exhibited a considerable increase with increasing the HAGB fraction from 53% for 8 passes to 66% for 16 passes without much change in the grain size. This is consistent with the results reported by previous researches[22–25] in that the high HAGB fraction is essential to extend ductility of equiaxed UFG materials since HAGB is beneficial for activating grain rotation[26] and grain boundary sliding/shearing[27–29] which lead to extended ductility in addition to its role as the effective dislocation source and sink.

3.3.2 Dislocation free length

As aforementioned, because ductility of the A sample with the lamellar structure is little affected by the HAGB fraction, other factor(s) controlling its ductility is to be explored. Jia *et al.*[30] and Yang *et al.*[31] suggested that the dislocation free length (L) of UFG grain elongated along the preferred orientation with respect to the stress axis is larger than that of equiaxed UFG grain. The larger L in the elongated grains is expected to result in extended ductility. Haouaoui *et al.*[9] estimated L by considering the geometrical change of an initial cubic element and the corresponding texture development during ECAP of OFHC Cu. In the case of repetitive route A, the initial cubic element elongates with an inclined angle θ_N with respect to the sample axis as shown in Fig. 7(a). In such a case, the inclined angle θ_N and the aspect ratio are expressed as

$$\tan\theta_N = \frac{1}{2N} \tag{1}$$

$$\text{Aspect Ratio} = \frac{a}{b} = \frac{(a_o/\sin\theta_N)}{(b_o \sin\theta_N)} \tag{2}$$

where N is the number of passage, a_o and b_o are the initial dimensions of the element ($a_o = b_o$ for the equiaxed), a and b are its longitudinal and transverse (i.e. grain thickness) dimensions respectively after N passage. The calculated θ_N and the aspect ratio for $N = 8$ and 16 are listed in Table 3. It should be reminded that this purely geometric consideration does not reflect the rearrangement of substructures such as dislocations and low angle boundaries at the grain (or element) interior. The substructural development may lead to the much smaller grain thickness and aspect ratio in actual. Haouaoui *et al.*[9] also reported that route A produces the texture similar to a rolling texture and the grain thickness direction (i.e. normal to the Z plane) is preferably oriented along the [313] direction in the case of OFHC Cu. Then, the

Table 3 Geometrical parameters for the configuration change of the element from cubic to lamella as a function of the number of passage for route A.

number of passage (N)	8	16
θ_N	3.58°	1.79°
aspect ratio	257	1024
ϕ	18.42°	20.21°
dislocation free length (L)	3.18b	2.89b

orientation relationship between the (111) slip plane and [313] direction viewed on the Y plane in the elongated grain can be schematically described as shown in Fig. 7(b); the angle between [111] and [313] is $\sim 22^\circ$ and ϕ ($= 22^\circ - \theta_N$) is the angle between the (111) slip plane and the longitudinal grain axis. The slip distance on the (111) plane can be approximated from the above geometric consideration. The calculated ϕ and L for $N = 8$ and 16 are also listed in Table 3. By assuming the (111) plane segment as the dislocation free length (L) as a first approximation in the 2 dimensional-wise as shown in Figs. 7(a) and 7(b), it decreased from $\sim 3.18b$ to $\sim 2.89b$, where b is the grain thickness, with increasing the number of passage from 8 to 16. This is consistent with the definite decrease of e_u of the A sample with increasing the number of passage described in Section 3.2. Accordingly, ductility of the A sample is likely to be more influenced by the dislocation free length (L) rather than the HAGB fraction. Meanwhile, the grain size and the equiaxed shape of the B sample remained nearly unchanged with increasing the number of passage from 8 to 16. Therefore, its dislocation mean free length would not change either with the number of passage and would not affect its ductility.

3.3.3 Post necking elongation

There is a substantial post necking elongation in both lamellar and equiaxed UFG OFHC Cu regardless of the number of ECAP passage. This observation is consistent with the previous study reported by Tsuji *et al.*[32] They found that post necking elongation of UFG 1100 Al and interstitial free steel, which were fabricated by the accumulative roll bonding process and so consisted of a pancake grain shape, is comparable to that of coarse grained counterparts. Accordingly, post necking elongation seems to be insensitive to the grain morphology, whether it is equiaxed, lamellar, or pancake. It is of interest to note in the present study that post necking elongation of the A8 sample was much larger than that of the B8 sample. However, while that of the A sample increased slightly with increasing the number of ECAP passage, that of the B sample increased considerably: post necking elongation of the B16 sample was as nearly same as that of the A16 sample. Accordingly, as stated in section 3.3.1, the HAGB fraction may affect post necking elongation of equiaxed UFG materials. Currently, the factors influencing post necking elongation of UFG materials (especially, for the lamellar UFG materials) are unclear and therefore it is to be further studied to enhance the total ductility of UFG materials. This is because post necking elongation occupies a much larger fraction of the total ductility of UFG materials than uniform elongation.

4. Summary

(1) Factors influencing room temperature tensile ductility of UFG OFHC Cu having the different grain morphologies, one the lamellar and the other the equiaxed which were prepared by ECAP of routes A and B_c respectively, were explored in association with their microstructural characteristics developed by ECAP.

(2) In the case of route A resulting in a lamellar UFG structure, the fractions of HAGBs and the grains less than 0.5 μm considerably increased with increasing the number of passage from 8 to 16. By contrast, an analysis shows that the dislocation free length decreased when the tensile loading axis is nearly parallel to the longitudinal lamellar grain axis. For route B_c producing an equiaxed UFG structure, the increment of the number of passage from 8 to 16 resulted in a definite increase of the HAGB fraction, but it did not alter the grain size distribution, and therefore the dislocation free length.

(3) Uniform elongation of the lamellar UFG OFHC Cu processed by route A decreased with increasing the number of passage from 8 to 16. Since the HAGB fraction increased but the dislocation free length decreased correspondingly, uniform elongation of the lamellar UFG OFHC Cu is to be more influenced by the dislocation free length rather than the HAGB fraction.

(4) Both uniform and total elongations of the equiaxed UFG OFHC Cu processed by route B_c increased with increasing the number of passage from 8 to 16. There was the corresponding increase of the HAGB fraction. But its dislocation free length was barely altered since the grain size as well as the equiaxed grain shape did not change. Accordingly, the HAGB fraction is to be the most influencing factor on ductility of the equiaxed UFG OFHC Cu.

Acknowledgments

This study was supported by a grant from the Basic Research Program of the Agency for Defense Development of Republic of Korea under the contract # UD070037AD.

REFERENCES

1) Y. Wang, M. Chen, F. Zhou and E. Ma: Nature **419** (2002) 912–915.
2) Y. M. Yang and E. Ma: Acta Mater. **52** (2004) 1699–1709.
3) K. Edalati, T. Fujioka and Z. Horita: Mater. Sci. Eng. A **497** (2008) 168–173.
4) J. Aldazabal and J. Gil Sevillano: Mater. Sci. Eng. A **365** (2004) 186–190.
5) C. C. Koch: Scr. Mater. **49** (2003) 657–662.
6) R. Z. Valiev: Met. Mater. Int. **7** (2001) 413–421.
7) Y. H. Zao, J. F. Bingert, X. Z. Liao, B. Z. Cui, K. Han, A. V. Sergueeva, A. K. Mukjerjee, R. Z. Valiev, T. G. Langdon and Y. T. Zhu: Adv. Mater. **18** (2006) 2949–2953.
8) R. J. Dowding, K. C. Cho, W. H. Drysdale, L. J. Kecskes, M. A. Minnicino and M. R. Staker: The AMPTIAC Quarterly **8** (2004) 71–78.
9) M. Haouaoui, I. Karaman and H. J. Maier: Acta Mater. **54** (2006) 5477–5488.
10) C. Xu, Z. Szàraz, Z. Trojanovà, P. Lukâč and T. G. Langdon: Mater. Sci. Eng. A **497** (2008) 206–217.
11) A. V. Panin, A. A. Pania and Y. E. Ivanov: Mater. Sci. Eng. A **486** (2008) 267–271.

12) L. J. Park, H. W. Kim, J. D. Yoo, C. S. Lee and K.-T. Park: Mater. Sci. Eng. A **527** (2010) 645–651.
13) Y. Iwahashi, J. Wang, Z. Horita, M. Nemoto and T. G. Langdon: Scr. Mater. **35** (1996) 143–146.
14) M. Furukawa, Y. Iwahashi, Z. Horita, M. Nemoto and T. G. Langdon: Mater. Sci. Eng. A **257** (1998) 328–332.
15) Y. Iwahashi, Z. Horita, M. Nemoto and T. G. Langdon: Acta Mater. **46** (1998) 3317–3331.
16) K. Oh-ishi, Z. Horita, M. Furukawa, M. Nemoto and T. G. Langdon: Metall. Mater. Trans. **29A** (1998) 2011–2013.
17) R. Z. Valiev and T. G. Langdon: Prog. Mater. Sci. **51** (2006) 881–981.
18) S. Lee and T. G. Langdon: Mater. Res. Soc. Poc. **601** (2000) 359–364.
19) S. Komura, Z. Horita, M. Nemoto and T. G. Langdon: J. Mater. Res. **14** (1999) 4044–4050.
20) A. Gholinia, P. B. Prangnell and M. V. Markushev: Acta Mater. **48** (2000) 1115–1130.
21) P. L. Sun, P. W. Kao and C. P. Chang: Metall. Mater. Trans. A **35** (2004) 1359–1368.
22) R. Z. Valiev: Nature Mater. **3** (2004) 511–516.
23) R. Z. Valiev, I. V. Alexandrov, T. C. Lowe and Y. T. Zhu: J. Mater. Res. **17** (2002) 5–8.
24) F. Dalla Torre, R. Lapovok, J. Sandlin, P. F. Thomson, C. H. J. Davis and E. V. Pereloma: Acta Mater. **52** (2004) 4819–4832.
25) Y. T. Zhu and T. G. Langdon: JOM **56** (2004) 58–63.
26) S. P. Joshi and K. T. Ramesh: Acta Mater. **56** (2008) 282–291.
27) H. Conrad: Mater. Sci. Eng. A **341** (2003) 216–218.
28) H. Conrad and K. Jung: Mater. Sci. Eng. A **391** (2005) 272–284.
29) H. Conrad and K. Jung: Mater. Sci. Eng. A **406** (2003) 78–85.
30) D. Jia, Y. M. Yang, K. T. Ramesh, E. Ma, Y. T. Zhu and R. Z. Valiev: Appl. Phys. Lett. **79** (2001) 611–613.
31) Y. M. Yang, E. Ma and M. W. Chu: Appl. Phys. Lett. **80** (2002) 2395–2397.
32) N. Tsuji, Y. Ito, Y. Saito and Y. Minamino: Scr. Mater. **47** (2002) 893–899.